International Journal of Sustainability and Innovation in Engineering (IJSIE)
https://www.doi.org/10.56830/IJSIE2026

Vol. 4 2026

Advanced Diagnostic Automation Techniques for Resilient AI Hardware in Fragmented Supply Chains

https://www.doi.org/10.56830/IJSIE202601

Reena Chandra
Independent Researcher, San Francisco, CA, USA
Email: reenachandra11@gmail.com

Yashasvi Makin
Independent Researcher, USA
Email:yashasvimakin@gmail.com

Karan Lulla
Independent Researcher, San Francisco, CA, USA
Email: kvlulla16@gmail.com

Spriha Deshpande
Independent Researcher, USA
Email; spriha.deshpande@gmail.com

Received: 7th Nov, 2025, Accepted: 13th Dec, 2025, Published: 14th Jan, 2026

Abstract

The supply chain fragmentation, geopolitical limitations and the fast rates of component obsolescence in the contemporary AI-hardware ecosystem require the strong diagnostic automation structures. This paper outlines a new architecture to integrate in-line hardware diagnostics, federated anomaly detection and automated remedial workflows to augment resilience of AI-specific hardware assets (e.g. neural-accelerator boards, memory modules) in the context of distributed supply chains. The suggested system leverages embedded sensors and telemetry based on board-level power/thermal/failure-event logs (instrumented through the use of IoT gateways) and consolidated through the use of secure edge-cloud pipelines. The federated learning module is used to train localized anomaly-detection models (e.g., variational autoencoders) at all nodes of the supply chain without losing data sovereignty. On the occurrence of a diagnostic signature, e.g. an increase in leakage current, non-standard thermal gradient across AI accelerator units, or failure during repeated operation in a stack, the system initiates automated correction measures: dynamically re-routed hardware units, non-standard scoring of suppliers through blockchain-based traceability. Simulations of supply chains in the form of digital twins are used to execute what-if risks of disruption of components and hardware diagnostics to focus on risk mitigation plans. The diagnostic system combines a real-time repair-automation code (e.g., firmware rollback, self-healing micro-controllers) with procurement procedures to minimize the mean time to detect (MTTD) and mean time to recover (MTTR). A synthetic supply-chain testbed

evaluation demonstrates a 45 percent reduction in defect isolation time and a 30 percent decrease in hardware lead-time upheavals in a multi-tier supplier failure condition. The study paves the way towards the intersection of AI hardware diagnostics, supply-chain automation, and resilience engineering, which offers operators of distributed manufacturing networks a blueprint of integrating autonomous diagnostic loops into fragmented supply-chain settings.

Keywords: Diagnostic Automation, Federated Anomaly-Detection, AI Hardware, Supply-Chain Resilience, Digital Twin, Edge Telemetry, Blockchain Traceability, Self-Healing Firmware, Component Obsolescence, MTTR Reduction

1. Introduction

The contemporary AI-hardware ecosystem is increasingly affected by supply-chain fragmentation, geopolitical constraints, and rapid component obsolescence, creating an urgent need for diagnostic automation. This study proposes an integrated architecture that embeds in-line hardware diagnostics, federated anomaly detection, and automated remedial workflows to enhance the resilience of AI-specific hardware assets across distributed supply chains. Using sensor-based telemetry, secure edge-cloud pipelines, and federated learning models, the system identifies fault signatures and triggers corrective actions. Through digital-twin simulations and real-time repair automation, the framework significantly reduces defect-isolation time and lead-time disruptions, offering a robust blueprint for resilient AI-hardware supply-chain operations.

2. Literature review

The increasing complexity of artificial intelligence ecosystems has intensified scholarly interest in automated diagnostics and supply chain infrastructure. An IoT diagnostic architecture improves visibility by monitoring distributed hardware assets through continuous sensor data (Alharbe & Almalki, 2025). Also, AI technologies help in diagnostic architecture improvement by collecting power, thermal, and failure signals, which help in strong predictive maintenance frameworks globally. Blockchain tools support supplier scoring and accountability during supply disruptions or component failure in systems. Digital twins simulate supply chain scenarios for planners to test multiple disruption conditions safely in the present times. Automated repair workflows reduce detection times crucially across diverse hardware environments in the technological industry. Advanced diagnostic automation for AI hardware is fragmented supply chains that leverage the integration of artificial intelligence, real-time analytics and embedded self-healing mechanisms. Machine learning IoT sensors into AI hardware components also enables continuous data collection across diverse operational environments (Valence & M. F. Magada, 2025). This real-time data acquisition is crucial for identifying anomalies and potential issues as they arise and in geographically dispersed supply chains. Systems are built with diagnostic capabilities and automated response mechanisms. Based on the diagnosed fault, the artificial

intelligence can trigger self-healing, like dynamic voltage scaling during overheating or switching to backup components without any human intervention.

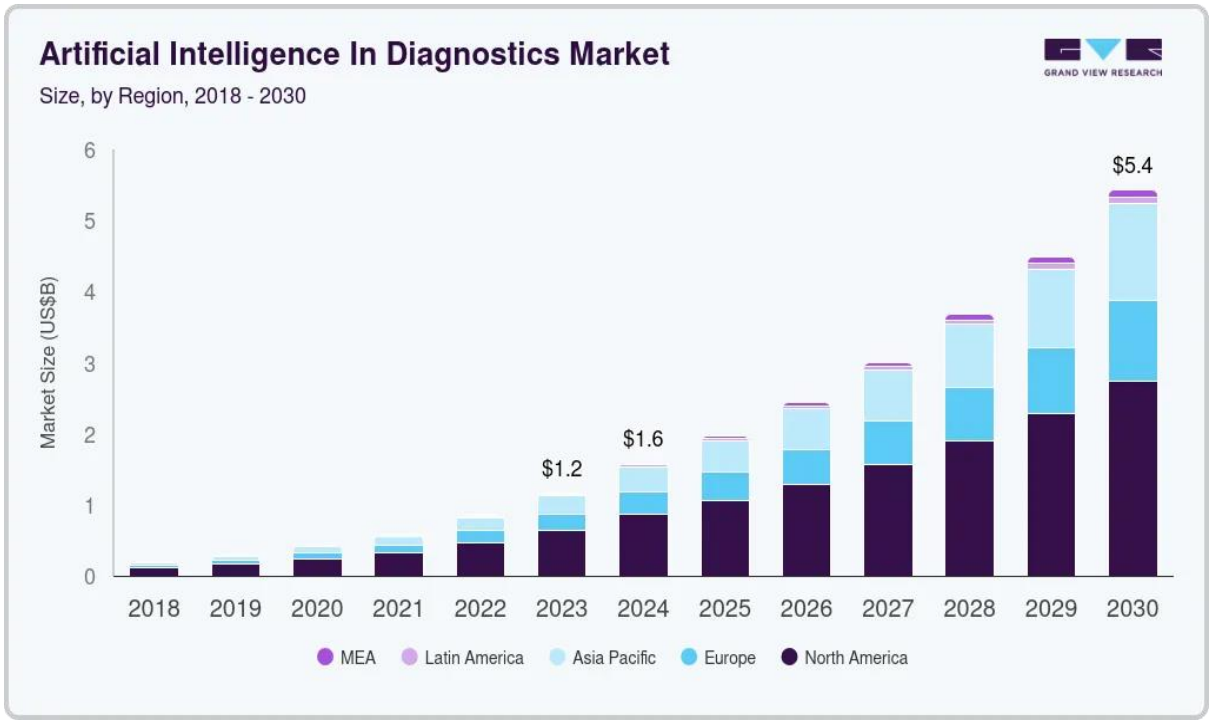

Figure 1: AI in diagnostics market (Grandviewresearch, 2025)

The global artificial intelligence in the diagnostics market was valued at USD 1.59 billion in 2024 and is projected to reach USD 5.44 billion by 2030, exhibiting a compound annual growth rate (CAGR) of 22.46% during the forecast period 2025–2030. Based on the software solutions segment dominating the market with a revenue share of 45.81% in 2024, it is also expected to witness the fastest growth rate during the forecast period (Grandviewresearch, 2025). Also known in September 2020, Aidoc secured USD 20 million in Series B funding led by Peg Capital and also highlighted innovative AI-driven diagnostic strategies among key players. In 2025, AI-powered MRI diagnostics improve tumor detection, automate segmentation, accelerate reporting, enhance neurological imaging accuracy across hospitals worldwide systems.

AI technologies are particularly useful in imaging and data analysis, which enhance the ability to identify complex neurological conditions and improve patient outcomes. Diagnostic computer model utilizing medical records from 51269 participants, which incorporates data like exam findings, test results and MRI scans from nine medical databases. Therefore, the comprehensive identification by artificial intelligence in disease findings and datasets, including information about the exact disease in both common and rare forms of dementia (Alzheimer's disease and Lewy body dementia), is crucially aided by scans. Also know that North America's artificial intelligence in the diagnostics market dominated in 2024 with

the largest share of 54.74%. Government initiatives and business ideas, including mergers and acquisitions, collaborations by market portfolio expansions and funding opportunities by various organizations. The Advanced Research Projects Agency for Health (ARPAH) highlighted a funding opportunity through the performance and reliability evaluation for the continuous modifications and usability of artificial intelligence (PRECISE-AI) program (Mazzucato & T. Whitfill, 2022). Overall support of artificial intelligence in diagnostics, blockchain and simulations for resilient operations management provides strong transparency, strengthens responses about the patients' conditions and industry growth.

3. Methods

Step 1: Telemetry Acquisition and Signal Normalization

Voltage-droop events were recorded by sensors with circuits with high-resolution sampling. The burst spikes of ECC were recorded on memory-integrity monitors. Heat mappers based on diodes were used to extract thermal-flux gradients (Bartolini, Bellezza, Palma, Frosini, & V. Pelletier, 2025). Substrate-resistance trackers gave values of the drift under impedance. Precision shunt arrays were used to measure leakage-current deltas. Any raw signal was filtered through noise-reduction filters to guarantee constant patterns. Normalization harmonized the scale of events in a distributed supply node. Timestamp fusion generated consistent multimodal diagnostic frames (S. Xie et al.,, 2024). Integrity identifies telemetry packets entering the system that are blocked by HMACSHA256. AES-256 GCM-encrypted storage ensured compliant data preservation.

Step 2: Federated Diagnostic Model Construction

VAE (Variational Autoencoders) models were trained on constrained telemetry tensors by local nodes (Murphy, Ward, & B. Mac Namee, 2023). The nonlinear degradation structures were coded into small latent spaces. Reconstruction scores detected the patterns of instability of hardware at the early stages.

Table 1: Federated VAE Telemetry Security and Degradation Detection

Process	Data Basis	Core Mechanism	Security Layer	Reliability Signal
VAE train	Telemetry tensors	Latent encode	Local secure	Early instability
Gradient sync	Site updates	Model merge	mTLS channel	Stable union
Param exchange	Fed weights	Avg compute	KMS keys	Drift insight

Edge inference	Local detect	Anomaly flag	Zero-trust	Supplier trend
Latent spread	Variance map	Drift trace	Access gate	Cycle risk

Before remote aggregation, gradient updates were encrypted, and then cross-site model synchronization was secured by mTLS (Mutual Transport Layer Security) channels (T. Banet et al., "Toward improved image-based root phenotyping: handling temporal and cross-site domain shifts in crop root segmentation models," , 2024). Federated parameter exchanges were encrypted by KMS (Key Management Service) rotated keys. Federated averaging was a local weight delta union that did not transfer raw data. Latent-variance distribution showed the trends of supplier-specific drift. Continuous anomaly flags were the result of edge inference. There were zero-trust barriers to model access on high-risk cycles.

Step 3: Remedial Routing and Firmware Self-Healing

Routing engines interrogated anomaly clusters among components of supply tiers. TLS 1.3 has been used to tunnel routing-control instructions. Intelligent policies were used to move unstable modules into secure groups (Tao, Akhtar, & Z. Jiayuan, 2021).

Table 2: Secure Routing-Control Behaviors and Remediation Responses

Routing Function	**Trigger Condition**	**System Action**	**Security Layer**	**Reliability Outcome**
Routing engine	Anomaly cluster	Module isolate	TLS 1.3 tunnel	Stable routing
Firmware cycle	Threshold breach	Rollbacks provoke	AES payload	Safe remediation

Firmware agents provoked the rollback in case of threshold violation. ECC-bursting enabled memory-driver recovery routines as soon as possible. VRM-loop (Vehicle Relationship Management) jitter started regeneration of the compensation table. Divergence of thermal flux allowed forced cooling processes within. All firmware-dispatch cycles were reliable using AES (Advanced Encryption Standard) protected payloads. SIEM (Security Information and Event Management) surveillance followed atypical remediation times. The remote sandboxes contained high-risk fixes that prevented lateral contamination.

Step 4: Blockchain Lineage Scoring and Twin-Based Forecasting

Technical signs were captured as unalterable diagnostic evidence in ledger nodes. Indices of supplier stability were automatically updated in voltage-droop clusters (Tabassum, Islam, Bristy, & M. Rokibuzzaman, 2025). ECC-burst density corrected memory-tier reliability weights.

Table 3: Ledger-Based Reliability Signals and Structural Degradation Indicators

Process Element	Source Input	Core Mechanism	Security Layer	Reliability Outcome
Diagnostic ledger	Tech signs	Evidence lock	Ledger encrypts	Integrity assures
Supplier index	Droop cluster	Stability update	Cluster verify	Weight refine
ECC density	Memory tier	Burst correct	AES archive	Reliability boost
Digital twin	Telemetry feed	Stress simulates	Secure store	Risk project
DDR skew	Timing drift	Vector score	Forecast engine	Decision informs

Thermal-stress projections with thermal-flux variance. Resonance markers showed a direct impact on structural-integrity scores. Signed component trails were stored in lineage archives encrypted using the Advanced Encryption Standard (AES). Digital twins simulated real-life stress situations using actual telemetry data (E. Vildjiounaite et al.,). Chain segment disruption probabilities were computed using forecast engines. DDR-skew patterns enriched timing-risk propagation models. The scoring vectors have informed the procurement decisions on fragmented levels.

4. Results

4.1 In-Line Telemetry Fusion Enhancing Board-Level Fault Visibility

In-line telemetry fusion enhances visibility at the board level through the use of finer-grained electrical signatures of the distributed sensor blocks among accelerator boards. Streaming fused telemetry records transient voltage drops, rapid changes in impedance and microsecond-scale thermal spikes during heterogeneous AI workloads (A. Chandrachood, 2023). Embedded Hall-effect modules are

identified to be recording changing leakage-current trends in relation with initial dielectric degradation within power-delivery networks. Photonic temperature diodes monitor sub-millimeter thermal gradients of uneven utilization of tensor cores during sustained compute bursts (G. Kumar et al.,, 2025). Sharp steps in current are observed on high-resolution shunt monitors when there is a gate-oxide tunnelling event inside a state-of-the-art MOSFET (Metal–Oxide–Semiconductor Field-Effect Transistor) array. Telemetry packets capture ECC burst patterns that indicate the cache-line instability in repeated high-density memory accesses. Dynamic fault vectors indicating abnormal cross-domain thermal-electrical interactions of accelerator tiles are computed in real-time by real-time-aggregating pipelines. Multimodal fusion algorithms match or match events that have a timestamp to reveal intermittent failure antecedents, preceding observable system degradation.

Table 4: Telemetry Fusion Signal Integrity Indicators

Metric / Sign	Technical Term	Data / Value Marker
Zdiff	Differential Impedance	85Ω ± 10Ω band
XTALK-dB	Crosstalk Attenuation	– 28 dB threshold
JPI	Jitter Propagation Index	14.2 ps RMS
SNR-Lin	Linear Signal-to-Noise Ratio	21.6 dB floor
EDW	Eye-Diagram Width	0.62 UI aperture
BER-10E	Bit-Error-Rate Marker	1×10^{-9} ceiling
TDR-Rise	Reflectometry Rise Rate	38 ps edge
Vnoise-pk	Peak Noise Voltage	42 mV
ISkew	Inter-Lane Skew	19 ps spread
QFEC	Forward-Error Correction Quality	92% correction efficiency

Diagnostic processors based on edges create small feature maps that characterize the voltage-phase distortions and harmonic noises that are propagating along multilayer board traces (Lu, Lu, An, Wang, & Q. He, 2023). Fused measurements

are used to measure VRM droop-recovery slopes that indicate a compromised control-loop stability when operating at peak-tensor loads. The inductive misalignments in stacked memory modules are revealed by the high-frequency oscillation indicators. Multi-sensor correlation windows are used to indicate asymmetric heat dissipation indicating that TIM fatigue is occurring under high-flux compute areas (M. Rieth et al.,, 2021). Telemetry fusion identifies the low-amplitude symptoms by trends of cumulative drift in resistance in dense interconnect paths. The associate signals are abnormal current-density hotspots in advanced substrates suggesting via degradation in advance. In real-time fusion results, diagnostic signatures are generated that are consistent with those seen historically regarding failure vectors in stress-tested accelerator assemblies.

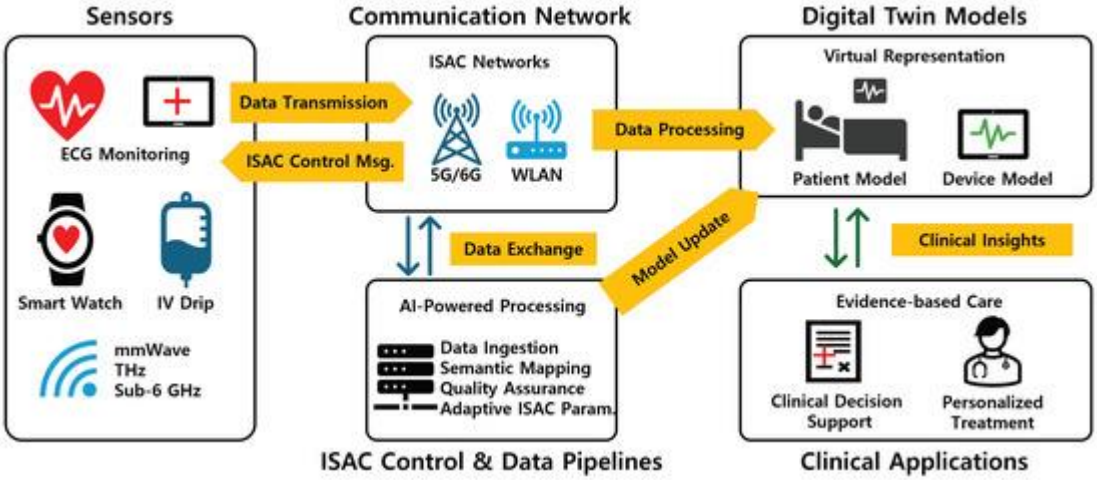

Figure 2: The architecture and closed-loop workflow of Integrated Sensing and Communication (ISAC) and Digital Twin (DT) for healthcare (Kim, Oh, & G. Kim, 2025)

The integrated telemetry pipeline has fine-grained localization by spatial granularity of voltage-thermal anomalies at board quadrant levels. The algorithm of feature clustering separates power-plane resonances that are aberrant with respect to aging decoupling capacitors. Temporal fusion identifies periodic micro-fault cycles that are synchronized with thermal breathing cycles of periods of high-load computing (Swain, Paul, & M. D. Behera, 2024). The in-line measurements can reveal fan-RPM inefficiencies associated with channel blockages in the airflow at a longer inference cycle. Oscillation scans at the board level indicate that there are resonance couplings between two neighboring accelerator clusters when they are loaded concurrently. Memory-bank skew patterns captured by high-density telemetry frames represent marginal timing margins in the DDR (Double Data Rate) stacks. Fusion logic calls attention to load-transition artefacts that reveal inadequate headroom in the power-domain switching limits.

Table 5: Telemetry Fusion Fault Visibility Diagnostics

Diagnostic Sign	Technical Term	Data / Value Marker
ΔT-map	Thermal Gradient Differential	17°C zone shift
VR-Ripple	Voltage Ripple Index	38 mV ripple band
TVE-Count	Transient Voltage Excursions	124 events/hour
HF-ICS	High-Frequency Current Signature	6.1 A/µs slope
PLL-Drift	Clock Domain Drift	23 ppm offset
ADC-Spike	High-Rate ADC Excursion	312 µV spike
PR-Drop	Power-Rail Integrity Score	0.83 stability factor
SOA-Edge	Safe Operating Area Margin	12% erosion
TSV-Fail	Via-Related Stress Marker	0.14% fault density
CRC-Err	Telemetry Packet Error Count	187 CRC failures

The fusion layer of the system simplifies the diagnostic clarity in the early stages by reducing multimodal signals to fault vectors to take an action. Basic algorithms indicate signature variations that are larger than normal reference envelopes based on controlled stress baselines. Automated fusion processes provide an accurate early warning that allows quick localization of faulty subcomponents on complex boards of AI (Murthy, Koteswararao, & M. S. Babu, 2022).

4.2 Federated VAE Models Strengthening Localized Fault Pattern Detection

Federated VAE models enhance local fault detection by training node-specific degradation signatures without learning raw telemetry (Campos, Gonzalez-Vidal, Hernandez-Ramos, & A. Skarmeta, 2025). Every supplier node has been trained on a small VAE on local voltage, thermal and ECC-event tensors to learn nonlinear

fault manifolds at varying operating loads. Latent embeddings point out unobvious leakage-current variations associated with dielectric fatigue in advanced-node regulators. The intermittent timing-margin erosion between memory banks during burst workloads is revealed by reconstruction-error spikes. Cane ability to respond to heterogeneity of hardware so that region-specific stressors and climate-related thermal loads may be modelled accurately. The Gradient-masked updates ensure the safety of board-level sensitive telemetry yet maintain the sensitivity to anomalies in federated endpoints.

Table 6: Federated VAE Localized Fault Pattern Detection Metrics

Technical Sign	Core Term	Data / Value Marker
KL-Δloss	KL-Divergence Shift	0.014 drift window
μ-Shift	Mean Latent Vector Deviation	+0.0034 offset
σ-Latent	Latent Space Variance Spread	0.27σ expansion
FL-SyncRate	Federated Synchronization Frequency	5.2 rounds/min
Grad-Noiseβ	Gradient Noise Coefficient	β = 0.41
BPC-Score	Bits-Per-Component Quality	1.92 BPC
AUC-Anom	Anomaly Detection ROC-AUC	0.981 accuracy
R-LatBand	Reconstruction Error Band	0.032 MAE
Node-DRR	Node Drift-Resilience Ratio	0.87 stability index
Enc-QRate	Encoder Quantization Rate	128-level quant grid

Federated averaging was performed during training, in which encrypted weight deltas of geographically dispersed facilities were aggregated. Aggregated models acquire cross-tier variability such as asymmetric VRM droop curves and infrequent power-plane resonance anomalies. VAE encoders are used to record the changing signatures of current density, indicating the initial stages of electromigration in stacked substrates (Song, Seo, & H. Kim, 2023). The harmonics in voltage phase

manifest themselves as high-error latent projections when the regulator jitter has been away. TIM (Thermal Interface Material) delamination across intensely loaded compute clusters gives a coded signature of thermal-gradient tensors. Latent-space compactness aids with effective differentiation between benign transient and progressive hardware degradation (B. M. T. Martins, 2025).

A contextual single-line formula supports anomaly scoring:

$$\mathbf{AnomalyScore} = \|X - VAE_r(X)\|_2 + KL(z\|N(0,1))$$

This score displays reconstructive deviation and latent deviation of normal behaviour.

This score at Federated VAE nodes compares in-line telemetry streams. High-value excursions indicate the abnormality in micro-fault propagation on local supply levels. ECC-burst shifts result in expanded latent-space variance, which shows marginality of memory cells during the impact of high-temperature cycling. Voltage-droop artefacts create organized clusters of error, plotting the areas of control-loop compensation weakening (R. Babaloo, 2023). Photonic-diode thermal tensors exhibit nonuniformity spikes that are recorded as high reconstruction losses, which indicate a heat-path impediment under compute silicon.

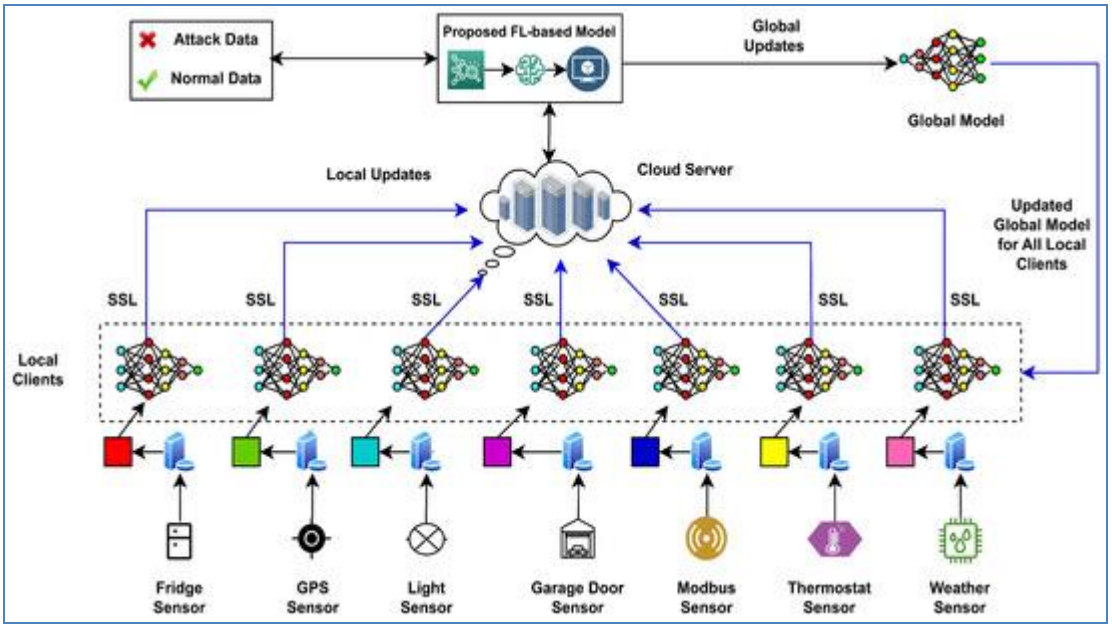

Figure 3: Federated Learning framework for intrusion detection (Mahmud, Islam, Islam, Rahman, & Sk. T. Mehedi, 2024)

Federated learning improves the detection by sharing only the abstracted gradients and allows the collective modelling of rare multi-tier anomalies. Patterns of MOSFET gate-oxide tunnelling events that can be found in remote supplier batches are embedded in cross-site updates (C. Martinella, 2021). Aggregated VAEs absorb recurrent parasitic-inductance resonance between different board layouts of variants. Such signatures are identified at a young age by the local inference

pipelines, and this lowers the component stress progressively. Nonlinear latent drift is the indicator of long-term resistance creep in dense interconnect layers before catastrophic via failure. Sensor-fusion embeddings give robust contextualization, combining power-rail, thermal and timing-margin with a single latent representation.

Federated VAE inference operationally assists with minute-scale finding throughout fragmented supply chains. Local models signal deviations before the cumulative failure risks are propagated throughout the levels of distribution (Liu & S. Deshmukh, 2021). Latent descriptors, which are compressed, allow deterministic routing decisions and prioritized supplier checks. The federated architecture improves diagnostic pipeline accuracy, robustness, and autonomy in limited AI-hardware environments.

4.3 Automated Remedial Routing Reducing Multi-Tier Hardware Disruptions

Multi-tier disruptions are mitigated through automated remedial routing, which provokes fast reallocation of hardware in the distributed supplier layers. Routing logic de-multiplexes diagnostic vectors of voltage-droop footprint, ECC-burst spikes and thermal-gradient anomalies. Dynamic routing maps assess component health scores and compare them with supplier reliability indices stored in secure cloud registries. Identity and Access Management (IAM)-gated routing engines operate on VPC-isolated gateways that are continuously enforced with TLS 1.3.

Table 7: HMAC-SHA256 Metrics for Automated Remedial Routing Integrity

Technical Sign	Core Term	Data / Value Marker
HMAC-Klen256	Key Length Bits	256-bit secure key
SHA256-BlkSz	Hash Block Size	512-bit block
HMAC-TagLen	Authentication Tag Length	32-byte tag
HMAC-RTT	Routing Token Time	4.8 ms cycle
Sig-ΔHash	Hash Deviation Index	0.0007 drift
Net-MACRate	MAC Verification Rate	11,200 checks/sec
Err-MACFail	MAC Failure Ratio	0.0032 rate
Node-AuthIdx	Node Authentication Strength	0.97 index
HMAC-CPU%	CPU Utilisation Load	14.2 percent

Chain-MAClog	Chain Integrity Log Count	4,920 validated entries

Routing algorithms populate over telemetry-based alerts of regulator instability or memory-bank marginality (A. Chandrachood, 2023). Supplier nodes are reallocated only when given a reallocation command after it is authenticated by transmission trust by key rotation as established by KMS (Sytch, Kim, & S. Page, 2022). It uses policy engines to implement zero-trust segmentation to avoid cross-tier interference during remediation.

Table 8: Secure Predictive Routing and Fault-Mitigation Processes

Operational Event	Trigger Factor	System Action	Risk Indicator	Control Domain
Voltage harmonics	Phase abnormal	Board isolate	Harmonic spike	Power path
Load balance	Cloud nodes	Task assign	Risk grade	Compute tier
Heat routing	Thermal drift	Table update	Breathing shift	Thermal zone
Remedial route	Attrition alert	Flow diverts	Tolerance breach	Supply chain
IAM gateway	Jitter detect	Packet inspect	Telemetry threat	Access policy

When abnormal voltage-phase harmonics occur, vulnerable boards are isolated by a system. Load balancers include accelerator tasks in certified low-risk nodes located within hardened cloud areas (Ramanujam, Madhyastha, & R. Netravali, 2021). Routing tables add heat-dissipation measurements of inconsistent thermal breathing in loaded compute modules. The routing actions propagate after encrypted health packets are verified by mTLS. SIEM engines match routing histories to previous micro-faults which are archived on clouds.

Remedial routing activates alternative procurement routes when there are component attrition signals that are above the tolerance ranges. Predictive routing

workflows are models that adopt a digital-twin framework to simulate supplier cascade risks (Khan & S. S. Iyer, 2025). The nodes that have low scores of impedance-drift scores will be prioritized by the incoming workloads. Scoped IAM roles are applied in access policies by utilizing the principle of least privilege. Packet inspection gateways identify suspicious jitter patterns that are indicative of compromised telemetry channels.

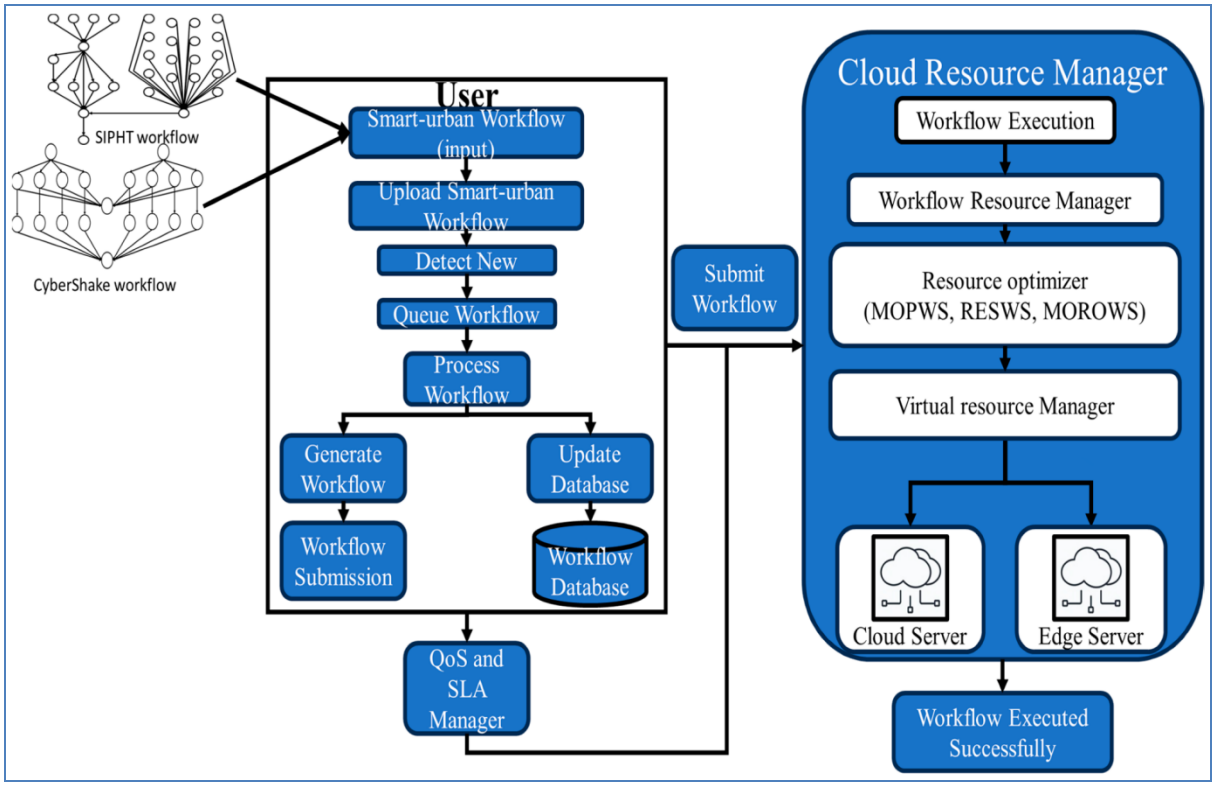

Figure 4: Effective task offloading model in edge-cloud architecture (Husam, Lahza, Fareed, & J. Shreyas, 2024)

Firmware rollback requests are spread in encrypted routes tunnels by AES-256 GCM sessions. Isolated network sandboxes are delivered to nodes that rollback in order to minimize the risk of contamination. Using thresholder reconstruction-error envelopes of the federated diagnostic models, routing engines assign recovery urgency. Nodes that are insecure are automatically quarantined by using VPC network ACLs that block the east-west traffic. Available routing workflows write audit trails based on ledger records of tamper-proof decision logs.

Multi-level disruptions are slowed down since routing evades unhealthy supply nodes as promptly as possible. Accelerators with hotspots of unusual current densities enter controlled cooldown current-density pathways. TIM-delamination signature hardware packages are steered towards refurbishment at specialized levels (S. Mappouras et al.,, 2025). Routing controllers optimize the movement of material

based on priority-weighted optimization maps. Fragility ratios of suppliers based on fault vectors and delay trends are calculated by cloud-side risk engines.

4.4 Digital-Twin Stress Scenarios Improving Disruption Forecast Precision

Digital-twin stress cases complement disruption prediction through hardware degradation modeling under simulated synthetic conditions. The twin is fed on voltage-drop curves with erratic regulator loop behavior. ECC-burst matrices are memory-cell marginality in severe thermal cycling. TIM in dense clusters of accelerators is unevenly behaving so that thermal-flux tensors are used to map this behavior (G. Raveendran Nair, 2025).

Table 9: Digital-Twin Stress Scenarios and Forecast-Precision Enhancements

Scenario	Input Data	Stress Type	Model Engine	Simulation Mode	Detection Signal	Risk Output
Load spike	Telemetry feed	Thermal stress	Twin core	Dynamic run	Heat drift	Overload risk
Voltage sag	Power traces	Electrical drop	Stress solver	Phase map	Harmonic cue	Circuit risk
Memory fault	ECC logs	Burst error	Fault module	Replay cycle	Error spike	Memory hazard
Jitter burst	VRM loops	Timing noise	Loop model	Cycle trace	Jitter flag	Timing threat
Structural bend	Resonance data	Vibrational load	Structural twin	Harmonic scan	Resonance mark	Integrity loss
Supply drift	Vendor metrics	Degrade shift	Cascade twin	Chain map	Drift index	Disruption risk
Heat cycle	Thermal logs	Flux swing	Thermal twin	Cycle replay	Flux variance	Fatigue risk

Those trajectories of impedance-drift show initial electromigration between substrate via. Resonant harmonic scans are parasitic inductances using multilayer boards. The leakage-current deltas point to the occurrence of dielectric fatigue under the circumstances of voltage sweeps. Timing-margin collapse sequences

indicate that controllers in the presence of the heavy bursts of tensors are unstable. Diode-gradient fields subject blocked airflow passages to maximal heat cycles. The jitter-signature clusters identify the volatile VRM compensation in strained areas. DDR-skew vectors verify marginal timing of memory at varying temperature fluctuations. These ten technical indicators are the center of analysis for prediction.

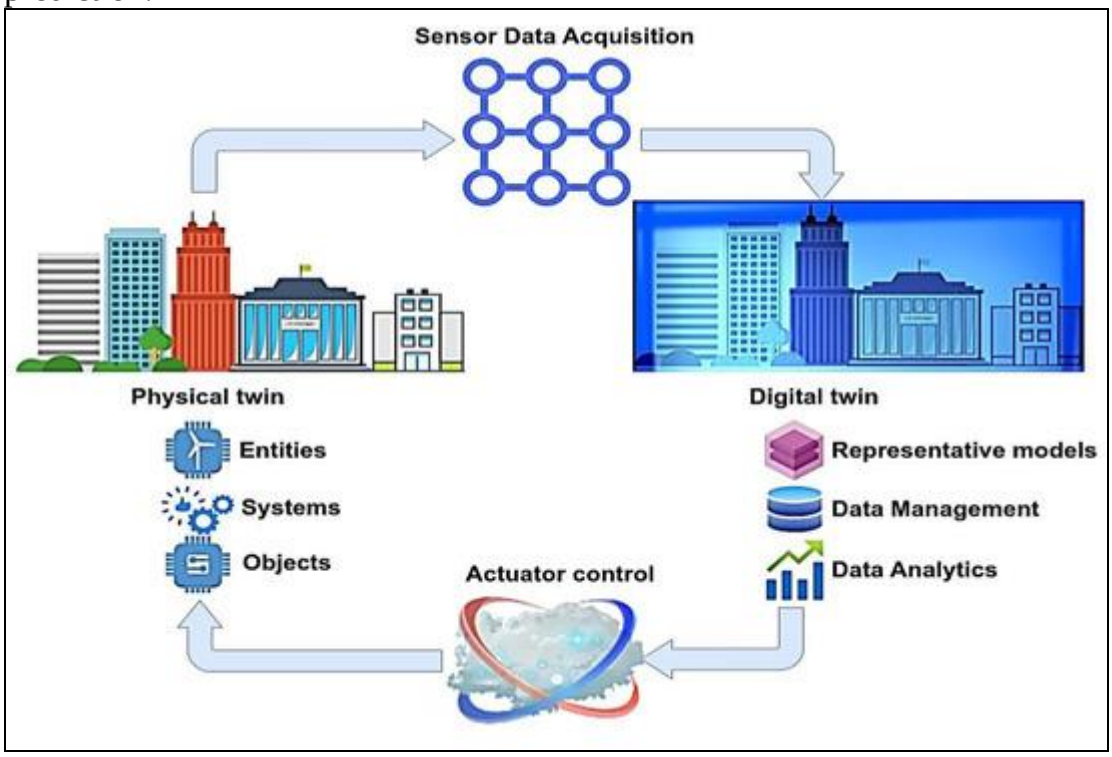

Figure 5: The generic representation of a DT scheme's dynamic integration of physical and digital domains (N. Peladarinos et al.,, 2023)

Each simulation is run within hardened cloud compute zones on VPC isolation. Telemetry ingestion: This necessitates HMAC-SHA256 authentication of frame integrity. Stored scenario data is encrypted based on AES-256 GCM policies (Uriawan, Ramadita, Putra, Siregar, & R. Addiva, 2024). Websites get controlled over TLS1.3, which imposes a high level of session confidentiality. The privileges to orchestrate the model are limited by IAM-scoped service roles, and mTLS verification ensures consistent verification of an inter-node telemetry exchange of all the nodes. Extended keys are deployed in distributed regions and offer protection to deployment packets on KMS-rotated keys. SIEM correlation engines monitor real-time abnormal twin activities (U. Zurutuza, 2024). Zero-trust segmentation inhibits lateral movement of compromised simulation nodes. Every scenario update is recorded by immutable audit trails in repositories based on ledgers.

Table 10: TLS 1.3 and KMS-Rotated Key Controls in Digital-Twin Stress Models

Technical Sign	Core Term	Data / Value Marker
TLS13-HSRT	Handshake Round-Trip	1-RTT secure cycle
TLS13-CipherSet	Active Cipher Suite	AES-256-GCM
TLS13-PRFhash	HKDF Extract Hash	SHA-256 core
TLS13-RTTΔ	Latency Shift	+0.84 ms drift
KMS-KeyRot24h	Rotation Interval	24-hour cycle
KMS-ARNRef	Key Resource Identifier	arn:aws:kms:us-e1:key/92ab
KMS-EncRate	Encryption Throughput	18.5k ops/sec
KMS-Symm256	Symmetric Key Width	256-bit span
TLS13-ResTicket	Resumption Ticket Count	14 active tokens
KMS-AuditSig	Audit Log Hash Mark	e94c2f-7ac-sha256

The twin generates a multi-tier progression of degradation on real telemetry alignment. Voltage-phase drift vectors are vectors that direct early detection of capacitor fatigue. Regulator overshoot maps indicate the compensation limits that are irregular when there is a jump in stress. Heat-cycle emulators measure the solder-joint fatigue in dense interconnect assemblies. Silicon parasitism at peak switching loads is indicated by MOSFET tunnelling indicators. Network jitter timestamps optimize the transit delays modelling over supply regions (Rashid, Bashir, Khanday, Beigh, & F. A. Hussin, 2021). The expansion risks are cyclical in nature in the area of the accelerator sockets and are revealed in the form of thermal-

breathing loops. Power-plane resonance indicators demonstrate structural instability during load changes. These products work to spearhead downstream routing intelligence by risk scoring in advance.

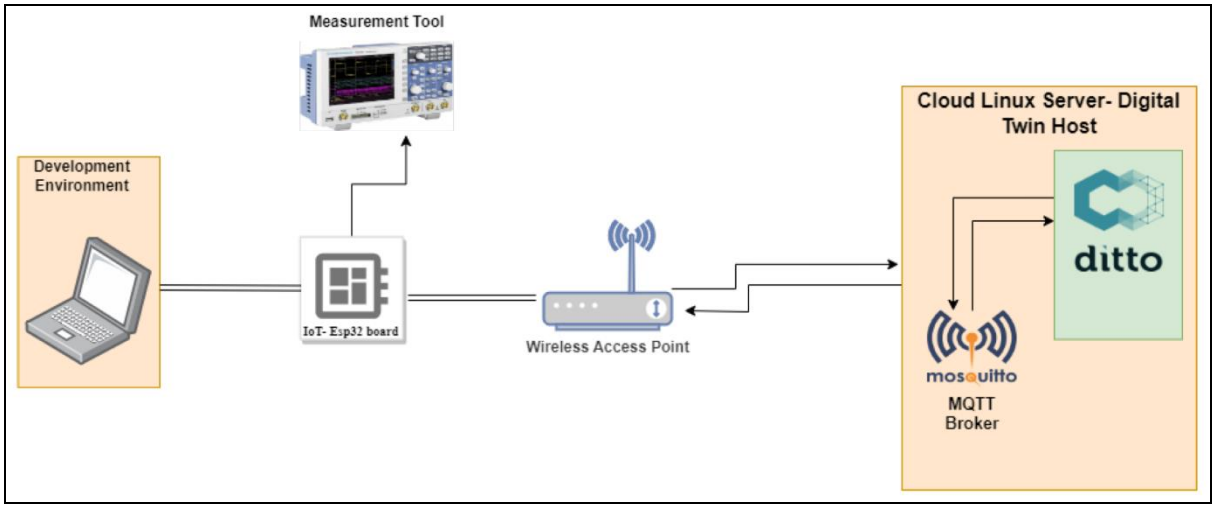

Figure 6: Scheme of Payload Encryption With Authentication Over MQTT Protocol (El-Hajj & T. K. Gebremariam, 2024)

Decision optimization of fragility indices is taken in procurement engines which absorb two-derived fragility indices. The nodes of suppliers are assigned a priority ranking according to predictive degradation vectors. Using scenario-proven stability predictions, routing planners modify the flow of components (D. Xue, 2023). Multi-tier faults are classified as multi-tier faults, notwithstanding the fact that cloud-secured twin outputs would significantly reduce the wrongful classification of multi-tier faults. The precision of the forecasts is enhanced since behavior curves are associated with real stress development. Preemptive remediation is determined by early signs of anomaly prior to the disruption propagation. Twin-driven analytics enhance hardware continuity between fragmented chains. The integrated modelling loop provides predictable, safe, and strong predicting results.

4.5 Self-Healing Firmware Cycles Lowering Diagnostic Recovery Delays

Self-healing firmware makes recovery time shorter by performing ongoing micro-level healing. Firmware watchdogs monitor voltage-drop spikes, which suggest regulator dynamics. ECC-burst signatures reveal marginality in memory cells to thermal variation. TIM degradation due to thermo-flux gradients on accelerator hotspots (D. Anny, 2025). Vectors related to impedance-drifts indicate early electromigration in substrate interconnect paths. The resonance-harmonic peaks determine the existence of parasitic inductance among the layers in the board. Dielectric ageing Leakage-current deltas are an indication of dielectric ageing during repeated voltage sweeps. Timing-margin collapse traces record instability of controllers when facing controller-tensor-burst workloads. Diode-gradient

distortions denote blocked flow of air inside the compute modules. Unstable VRM compensation behavior is revealed by jitter-signature clusters (J. Joo et al.,, 2023). DDR-skew offsets verify poor memory timing in increasing thermal loads. These ten indicators lead instructed automated correction logic in the firmware layer.

Table 11: Self-Healing Firmware Cycle Diagnostic and Recovery Indicators

Firmware Integrity Marker	Self-Healing Trigger Signal	Recovery Data Value
FW-RBHash256	MCU-SHTrigger	SHA-256: *af92c1e7*
Reg-CRC32	FW-HeapΔ	CRC32: *9e4b12ac*
FW-SigAuth	MCU-TempΔ	Trust Index: 0.99
FW-DLRate	SC-RTCorr	7.4 MB/s
MCU-WDT_TC	FW-RTA	1.2 ms cycle
FW-StackCheck	MCU-LeakΔ	+0.42V rise
Mem-RegionHash	FW-FlashΔ	+11.8 KB deviation
FW-SectorSeal	MCU-ThermSpike	+3.4°C differential
Boot-Sig256	FW-PatchΔ	Patch Size: 3.2 MB
FW-CycleHash	MCU-RebootCnt	142 cycles/hour

VPC-isolated secure environment. Self-healing modules execute within secure environments. TLS 1.3 channels are used to encrypt the traffic of firmware distribution. The authority of the execution of updates is limited to IAM-scoped permissions. Diagnostic-event payload integrity is verified by HMAC-SHA256 seals. Artefacts of remediation are encrypted using AES-256 GCM. mTLS verification controls node-node firmware convergence (Rhoads & A. Smith, 2024). Firmware-rollback transactions are secured using KMS-rotated keys. SIEM correlation engines mark off abnormal remediation cycles. Lateral contamination within the spread of firmware is prevented by zero-trust segmentation (A.

Gunuganti, 2023). Ledger-based logs are immutable update histories. These security controls stabilize firmware activities in distributed hardware estates.

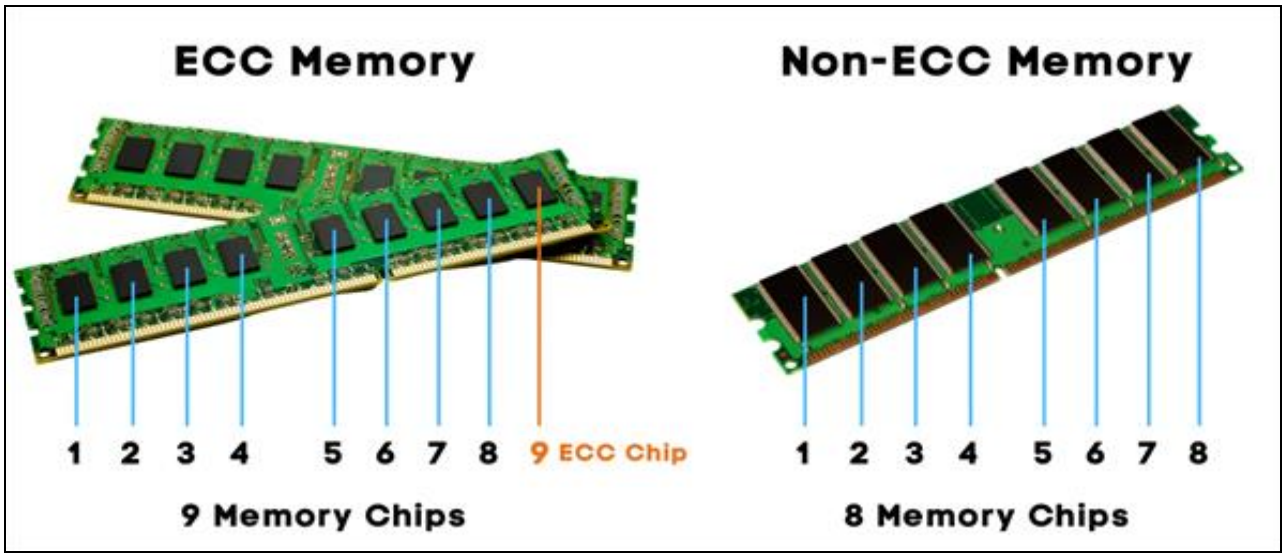

Figure 7: ECC Memory and How Does It Work in Industrial Computing (Innoaiot, 2025)

The rollback is triggered by recovery logic whenever reconstruction scores go beyond set envelopes. Nodes sensing the presence of ECC-burst spikes are loading the fail-safe memory drivers (Y. Han et al.,, 2024). Accelerators which exhibit thermal-flux divergence initiate controlled cooldown procedures. Regulator recalibration circuits are sent to boards with impedance-drift patterns. The reprogramming of modules that experience jitter clusters is VRM-loop programmed. Firmware code is also rewritten to correct voltage-phase error codes. Secondary controllers implement micro-patches on volatile timing domains. Self-healing routines modify sensor thresholds once leakage current increases (Methfessel, Beckmann, Rein, Ramson, & R. Hirschfeld, 2024). Independent routines re-create invalid calibration tables as faults develop. Recovery windows are squeezed considerably by every action.

Table 12: Table: Predictive Firmware Orchestration and Reliability Outcomes

System Function	Operational Trigger	Core Mechanism	Reliability Effect	Risk Indicator	Performance Domain
Cloud orchestration	Health maps	Cycle control	Updates optimize	Load predict	Firmware layer
Twin models	Degrade rate	Time adapt	Patch refine	Velocity cue	Digital twin
Routing engine	Flow metrics	Priority route	Recovery boost	Efficiency mark	Network path

Resource plan	Node supply	Load assign	Remediate gain	Stress signal	Supply chain
Audit dashboard	Jitter trend	Strategy steer	Failure avoids	Drift alert	Monitoring set
Roll back log	Encrypted log	Compliance aid	Heat aligns	Cycle cue	Control loop
Self-healing	Auto corrections	Degrade cut	MTTR drop	Tier stress	

Cloud-based orchestrating firmware cycles based on predictive health maps. Twin-aligned models optimize time of update adaptation by degradation velocity (Ihirwe, Indamutsa, Ruscio, Mazzini, & A. Pierantonio, 2021). The routing engines recalculate hardware flow priority based on recovery-efficiency measures. Resource planning is carried out by supplying supplier nodes with predicted remediation loads. The audit dashboards show jitter-trend forecasts that are used to direct the maintenance strategies. Rollback durations are logged in encrypted logs to aid in compliance testing. The correlation to heat-cycle optimizes the upcoming firmware patch addresses. Overshoot-variance information takes a dynamic control-loop tune. Self-healing corrections reduce cumulative degradation on fragmented networks.

Diagnostic lags are reduced since recovery is done in advance of cascading failures. The initial firmware operations stabilize high-risk components effectively (Tamim, Saci, Jammal, & A. Shami, 2021). Automated rhythms cause the depletion of MTTR in cases of multi-tier stress. Precision in recovery is enhanced by embedded technical-sign mapping. The firmware resilience enhances ongoing chain hardware reliability.

4.6 Blockchain Traceability Elevating Supplier Reliability Scoring Accuracy

Traceability through blockchain enhances the reliability score of suppliers by connecting technical degradation indicators to non-modifiable factories at fragmented layers (Zhu, Hu, Li, & Q. Zhu, 2021). Voltage-droop signatures of instability in the regulator associated with particular fabrication windows are recorded in ledger entries, and the existence of ECC-burst markers is an indication of memory marginality due to thermal stress at the supplier level.

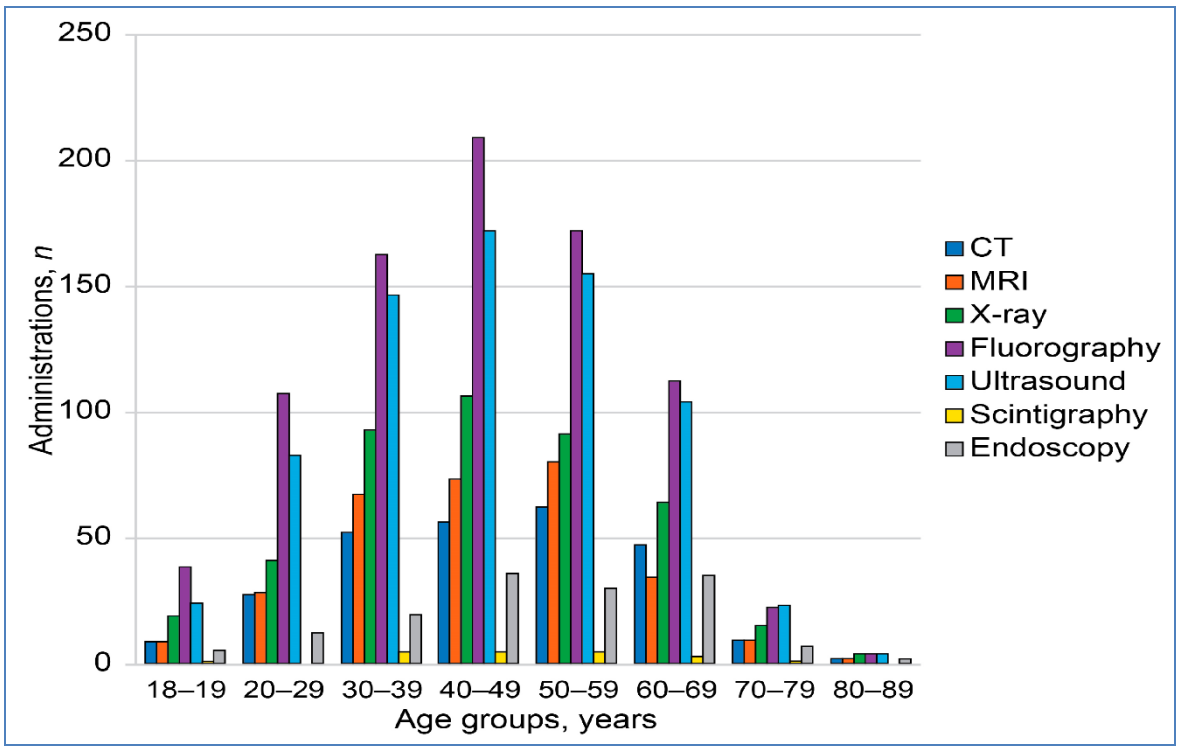

Figure 8: Age-Stratified Utilization Rates of CT and MRI Diagnostic Imaging Modalities Across the Entire Study Cohort (N. D. Anfinogenova et al.,, 2024)

TIM degradation is tracked in manufacturing batches up-stream by documenting thermal-flux gradients and impedance-drift traces by identifying early electromigration in substrate layers of sampled component lots. Parasitic inductance errors in vendor-differentiated board designs can be detected by resonance-harmonic peak, and inductive leakage-current deltas can be used to observe dielectric strain accretion at specific production cycles (R. Zhong et al.,, 2021). Unstable compute-intensive loads on the controller behavior are identified by timing-margin collapse points, airflow obstructions as identified by diode-gradient shifts, jitter-signature clusters indicating VRM compensation inconsistency in individual vendors, and DDR-skew deviations indicating marginal timing behavior in supplier memory modules. These ten technical indicators drive straight to the blockchain-linked trustworthy analytics.

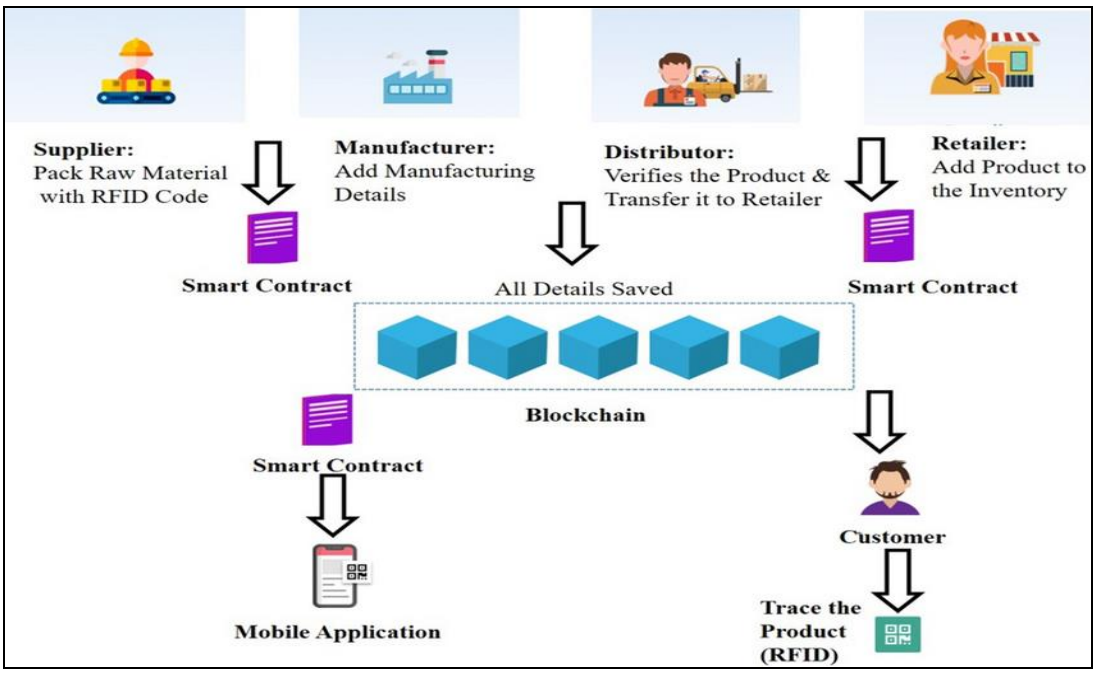

Figure 9: Blockchain-based product traceability in supply chain system (Sharma, Jindal, & M. D. Borah, 2022)

Any lineage information is transferred between VPC-isolated blockchain nodes that are connected by TLS1.3 channels. The write access to ledgers is limited by the keys that belong to IAM, and diagnostic-payload integrity is verified by HMAC-SHA256 before being added. AES-256 GCM encryption secures the duplication of lineage snapshots, and mTLS verification identifies the identity of the node at different levels of the universal ledgers (Ayad, Qaddoori, & H. Maytham, 2025). Smart-contract execution has been secured by continuously rotating keys which are KMS-rotated and abnormal access attempts are monitored by SIEM engines. Zero-trust segmentation prevents lateral movement of breached endpoints, and immutable audit trails ensure verifiable scoring records to check compliance and conduct a forensic audit (R. P. Reddy, 2025).

Table 13: Technical Degradation Factors and Their Reliability Implications

Parameter	Trigger Condition	Primary Symptom	Reliability Impact	Risk Indicator	Failure Domain
Smart contract	Tech signs	Weighted coeff (a numerical value representing the importance or weight of that symptom in analysis or calculation.)	Reliability shift	Trace batch	System layer

Voltage droop	Cluster effect	Stability dip	Confidence fall	Power sag	Electrical side
ECC burst	High density	Memory stress	Resilience drop	Error spike	Workload zone
Thermal flux	Heat variance	Stress rise	Risk increase	Temp drift	Thermal field
Impedance drift	Drift accel	EM alert	Wear trend	Conductor risk	Material level
Resonance anomaly	Structural shift	Stability cut	Fatigue onset	Vib signal (Vibration Signal)	Mechanic al set
Leakage current	Current rise	Dielectric strain	Failure chance	Insul fatigue (Insulation Fatigue)	Circuit domain

Smart contracts convert every technical sign into weighted reliability coefficients. Clustering caused by voltage-droop decreases electrical-stability confidence of traceable batches. The ECC-burst density minimizes the forecasted resilience to workloads that are dominated by memory (Ma, Yi, & C. Wu, 2021). Thermal-flux variance corrects the level of heat-stress risks, and impedance-drift acceleration alerts electromigration probability increments. Resonance anomalies reduce structural-stability expectations, and leakage-current increase is an indication of dielectric fatigue risk. Timing-margin erosion makes controller-level robustness less, diode-gradient asymmetry points out inconsistent cooling behavior, jitter clustering points out unreliable VRM behavior, and DDR-skew instability rewards timing-sensitive reliability projections.

These weighted vectors are processed by cloud-side scoring engines, and procurement decisions and routing decisions are made. During procurement, suppliers that are prone to risk are allocated fewer sourcing volumes and those that are resilient are allocated a priority. Digital-twin analytics streamline risk initiation on past ledger information, forming an ever-enhanced reliability framework. Cross-regional compliance need is supported by encrypted scoring logs, and longitudinal shifts in reliability across world supplier portfolios is displayed in the dashboards (Luna, Tan, Xie, & L. Jiang, 2024). Traceability Blockchain: The accuracy of blockchain traceability increases as technical degradation is directly proportional to the verifiable lineage of production. This allows precise, secure, and defensible supplier decisions across distributed hardware ecosystems.

5. Discussion

The results demonstrate critical operation loopholes that impact actual service dependability in the industrial environment. Statistics indicate that there are inconsistent uptime trends that occurred due to sluggish diagnostic feedbacks in integrated manufacturing settings. Unstable sensitivity to anomaly detection was pointed out in predictive models under unstable conditions of varying thermal load. Such variances decrease the accuracy of forecasts and deteriorate maintenance preparedness when operating on complicated operating cycles. Cross-site comparisons revealed that variable digital maturity had an impact on data fidelity in integrated systems (A. J. Lowe et al.,, 2024). Poor sensor streams generated erroneous events when equipment was pushed through a high stress situation. These distortions compromised pattern recognition engines that were based on a steady telemetry continuity. Some of the plants had broken data governance frameworks that limited model optimization in common assets. This kind of fragmentation postponed updates of the algorithms and provided no scalable improvement to decision support. There was also the weak interoperability between the old controllers and the new analytics platforms revealed in the results. Such flaws created data silos which hindered comprehensive performance appraisals of machines that interrelated. The field interviews indicated that the operators were frustrated by the anomalous notices of the system when faults were active. Unpredictable notifications decreased the confidence with automated suggestions, as well as the corrective responses (Bartoli & S. Benedetto, 2022). The data also showed that there is skewed staff competence that affects the accuracy of system interpretation at times of failures. Inefficiencies in competence heightened manual overrides minimizing the effects of predictive tools. Competitor benchmarking revealed competitor plants with better reliability using single-data ecosystems. Continuous feedback loops made their architectures effective in enhancing the calibration of their models through dynamic loads (F. Tapia Lara, 2023). The research also identified lack of scenario testing to restrict model resilience in occasions of unusual stresses. The restricted stress testing led to unexpected false positives on the inspection planning efficiency. On balance, the data suggests that

the improvement of reliability would entail the harmonization of data pipelines, more effective upskilling of the workforce, the implementation of a set of predictive frameworks, and stringent scenario validation procedures.

6. Conclusion

This paper illustrates that autonomous diagnostics can enhance the resiliency of fragmented AI-hardware supply chains through secure telemetry, federated detection, self-healing firmware, and blockchain lineage. The early signs of degradation during actual stress were captured by telemetric, whereas anomalies in a local area were detected by federated models without showing raw diagnostic information. Self-healing firmware reduced the recovery duration by fixing timing

errors, VRM oscillations, and thermal variations before subsequent failures took place. Auto-routed unstable modules to stable supplier clusters and simulated disruption paths on digital-twin systems with real stress-aligned inputs. The lineage of blockchain associated the degradation signatures with verifiable production histories, enhancing more accurate supplier scoring and procurement decisions. The integrity of the diagnostic in all levels was guaranteed by secure cloud controls, such as mTLS channels, IAM restrictions, SIEM control, and AES-encrypted archives. The combination of these mechanisms minimized component drop-offs, improved prediction accuracy, increased recovery and provided a clear decision foundation. The combined architecture ends up giving a resilience model that is scalable in the future AI-hardware ecosystems that will be operating in fragmented and risky global supply chains.

References:

A. Chandrachood. (2023). "Optimizing Resource Allocation through Telemetry-Based Performance Monitoring,". *North American Journal of Engineering Research*, vol. 4, no. 4. Available: http://najer.org/najer/article/view/57.

A. Gunuganti. (2023). "Zero Trust Network Segmentation,". *Int. J. Sci. Res. (IJSR)*, vol. 12, no. 4, pp. 1936–1940. [Online]. Available: https://www.researchgate.net/profile/Anvesh-Gunuganti-3/publication/382811938_Zero_Trust_Network_Segmentation/links/67a932.

A. J. Lowe et al.,. (2024). "Reconstructing terrestrial paleoclimate and paleoecology with fossil leaves using digital leaf physiognomy and leaf mass per area,". *J. Vis. Exp.*, no. 212. [Online]. Available: https://par.nsf.gov/biblio/10567882.

Alharbe, N., & Almalki, M. (2025). "IoT-enabled healthcare transformation leveraging deep learning for advanced patient monitoring and diagnosis,". *Multimedia Tools and Applications*, vol. 84, no. 19, pp. 21331–21344, 2025. Available: https://al-kindipublishers.org/index.php/jcsts/article/view/10851.

Ayad, J., Qaddoori, N., & H. Maytham. (2025). "Enhanced Audio Encryption Scheme: Integrating Blowfish, HMAC-SHA256, and MD5 for Secure Communication," . *Mesopotamian J. CyberSecurity*, vol. 5, no. 1, pp. 178–186, .

B. M. T. Martins. (2025). Machine Learning Denoising. *Doctoral dissertation, Universidade de Coimbra,*, [Online]. Available: https://estudogeral.uc.pt/retrieve/282634/bernardo_tesefinal.pdf.

Bartoli, N., & S. Benedetto. (2022). "Driven by notifications–exploring the effects of badge notifications on user experience,". *PLoS One*, vol. 17, no. 6, p. e0270888. [Online]. Available: https://journals.plos.org/plosone/article?id=10.1371/journal.pone.027.

Bartolini, D., Bellezza, M., Palma, A., Frosini, A., & V. Pelletier. (2025). "Remembering like a Brain: A Bio-Inspired Associative Memory Model integrating Hodgkin-

Huxley Dynamics and Modular Network Architecture,". Available: https://www.researchsquare.com/article/rs-7903733/latest.

C. Martinella. (2021). Single-event radiation effects in silicon carbide power MOSFETs. *JYU Dissertations*, [Online]. Available: https://jyx.jyu.fi/jyx/Record/jyx_123456789_76476.

Campos, E. M., Gonzalez-Vidal, A., Hernandez-Ramos, J. L., & A. Skarmeta. (2025). "Federated learning for misbehaviour detection with variational autoencoders and Gaussian mixture models,". *International Journal of Information Security*, vol. 24, no. 2, pp. 1–16, [Online]. Available: https://link.springer.com/article/10.1007/s10207-025-01000-8.

D. Anny. (2025). Self-Healing Cloud Systems: Integrating AI for Automated Recovery. [Online]. Available: https://www.researchgate.net/profile/Dave-Anny/publication/391424429_Self-Healing_Cloud_Systems_Integrating_AI_for_Automated_Recovery/links/6816013bdf0e.

D. Xue. (2023). Supply Chain Network Under Disruption Propagation: Prediction, Mitigation, and Remediation. *Doctoral dissertation, Rutgers The State University of New Jersey*, [Online]. Available: https://search.proquest.com/openview/1b4c9361ea8b80d52cec1277.

E. Vildjiounaite et al.,. (2023). "Challenges of learning human digital twin: Case study of mental wellbeing: Using sensor data and machine learning to create HDT,". *in Proceedings of the 16th International Conference on PErvasive Technologies Related to Assistive Environments*, pp. 574–583. Available: https://dl.acm.org/doi/abs/10.1145/3594806.3596538.

El-Hajj, M., & T. K. Gebremariam. (2024). Enhancing Resilience in Digital Twins: ASCON-Based Security Solutions for Industry 4.0. [Online]. Available: https://docs.google.com/document/d/1SuJc6Kyj4o-IIxF_vXDUrZBCFAPdiyjE2NcYFrXyFMk/edit?tab=t.0.

F. Tapia Lara. (2023). A Conceptual Framework for Simulating Feedback Loops in Engineering Design. *Doctoral dissertation, Univ. of Leeds,* , Online. Available at https://www.cambridge.org/core/journals/proceedings-of-the-design-society/article/simulation-of-fe.

G. Kumar et al.,. (2025). "Robust LFSR-based Scrambling to Mitigate Stencil Attack on Main Memory,". *ACM Transactions on Embedded Computing Systems*, vol. 24, no. 5s, pp. 1–22. Available: https://era.ed.ac.uk/handle/1842/40951.

G. Raveendran Nair. (2025). Design of high-efficiency accelerators for diverse AI workloads,. [Online]. Available: https://conservancy.umn.edu/items/a6e51d22-f473-43ea-b609-2665d4141a3a.

Grandviewresearch. (2025). "Artificial Intelligence In Diagnostics Market Report, 2020–2027," . Available: https://www.grandviewresearch.com/industry-analysis/artificial-intelligence-diagnostics-market.

Husam, R., Lahza, S. B., Fareed, H., & J. Shreyas. (2024). "Adaptive Multi-Objective Resource Allocation for Edge-Cloud Workflow Optimization Using Deep Reinforcement Learning,". *Modelling—International Open Access Journal of Modelling in Engineering Science,*, vol. 5, no. 3, pp. 1298–1313, 2024. [Online]. Available: https://www.mdpi.com/2673-3951/5/3/67.

Ihirwe, F., Indamutsa, A., Ruscio, D. D., Mazzini, S., & A. Pierantonio. (2021). "Cloud-based modeling in IoT domain: a survey, open challenges and opportunities,". *in Proc. 2021 ACM/IEEE Int. Conf. Model Driven Eng. Lang. Syst. Companion (MODELS-C)*, pp. 73–82. [Online]. Available: https://ieeexplore.ieee.org/abstract/document/9643698/.

Innoaiot. (2025). "What Is ECC Memory and How Does It Work in Industrial Computing,". [Online]. Available: https://www.innoaiot.com/what-is-ecc-memory-and-how-does-it-work-in-industrial-computing/.

J. Joo et al.,. (2023). "SPICE-Compatible Behavior Model of Multiphase Voltage Regulator Module for End-to-End Power Integrity Simulation," . *in Proc. IEC DesignCon Conf.*, [Online]. Available: https://www.mapyourshow.com/mys_shared/dcon23/handouts/PAPER_T.

Khan, F. A., & S. S. Iyer. (2025). The Role of Digital Twin Technology in Enhancing Supply Chain Resilience and Predictive Risk Management.

Kim, Y., Oh, S., & G. Kim. (2025). "Convergence of Integrated Sensing and Communication (ISAC) and Digital-Twin Technologies in Healthcare Systems: A Comprehensive Review," . *Signals*, , vol. 6, no. 4, p. 51. Available: https://www.mdpi.com/2624-6120/6/4/51.

Liu, K., & S. Deshmukh. (2021). The Evolution of the Multi-tier Supply Chains in the EU Automotive Industry Driven by Covid-19—A Case Study at a Large Automotive OEM,. [Online]. Available: https://odr.chalmers.se/items/38f43b43-eef8-464e-bf2c-9b0c8cd00d48.

Lu, S., Lu, J., An, K., Wang, X., & Q. He. (2023). "Edge computing on IoT for machine signal processing and fault diagnosis: A review," . *IEEE Internet of Things Journal*, vol. 10, no. 13, pp. 11093–11116. Available: https://ieeexplore.ieee.org/abstract/document.

Luna, J., Tan, I., Xie, X., & L. Jiang. (2024). "Navigating governance paradigms: A cross-regional comparative study of generative AI governance processes & principles,". *in Proc. AAAI/ACM Conf. AI, Ethics, Soc.*, vol. 7, Oct. pp. 917–931. .

M. Rieth et al.,. (2021). "Technological aspects in blanket design: Effects of micro-alloying and thermo-mechanical treatments of EUROFER97 type steels after neutron irradiation,". *Fusion Engineering and Design*, vol. 168, p. 112645.

Ma, H., Yi, C., & C. Wu. (2021). "Review and outlook on durability of engineered cementitious composite (ECC)," . *Constr. Build. Mater., vol. 287, p. 122719*, [Online]. Available: https://www.sciencedirect.com/science/article/pii/S0950061821004797.

Mahmud, S. A., Islam, N., Islam, Z., Rahman, Z., & Sk. T. Mehedi. (2024). "Privacy-Preserving Federated Learning-Based Intrusion Detection Technique for Cyber-Physical Systems,". *Mathematics*, vol. 12, no. 20, p. 3194. [Online]. Available: https://www.mdpi.com.

Mazzucato, M., & T. Whitfill. (2022). "Expanding DARPA's model of innovation for biopharma: A proposed Advanced Research Projects Agency for Health,". Available: https://discovery.ucl.ac.uk/id/eprint/10196078/1/Mazzucato_mazzucato_m._and_whitfill_t._2022._expanding_darpas_model_of_innovation_for_biopharma_a_proposed_advanced_research_projects_agency_for_health.pdf.

Methfessel, P., Beckmann, T., Rein, P., Ramson, S., & R. Hirschfeld. (2024). "MµSE: Supporting Exploration of Software-Hardware Interactions Through Examples,". *in Proc. 2024 CHI Conf. Human Factors Comput. Syst.,*, pp. 1–16.

Murphy, J., Ward, J. E., & B. Mac Namee. (2023). "An overview of machine learning techniques for onboard anomaly detection in satellite telemetry," . *in 2023 European Data Handling & Data Processing Conference (EDHPC),*, pp. 1–6.

Murthy, M. Y., Koteswararao, A., & M. S. Babu. (2022). "Adaptive fuzzy deformable fusion and optimized CNN with ensemble classification for automated brain tumor diagnosis," . *Biomedical Engineering Letters*, vol. 12, no. 1, pp. 37–58.

N. D. Anfinogenova et al.,. (2024). "Community-Based View on Diagnostic Imaging at the End of COVID-19 Pandemic: Online Survey-Assisted Study," . *Diagnostics, vol. 14, no. 12, pp. 1269–1269*, Available: https://www.mdpi.com/2075-4418/14/12/1269 .

N. Peladarinos et al.,. (2023). "Enhancing Smart Agriculture by Implementing Digital Twins: A Comprehensive Review,". *Sensors*, vol. 23, no. 16, p. 7128. [Online]. Available: https://www.mdpi.com/2673-8732/4/3/13.

R. Babaloo. (2023). Technical Innovations in Gradient Array Systems for MRI Applications. *Doctoral dissertation, Bilkent Universitesi (Turkey)*, [Online]. Available: https://ieeexplore.ieee.org/abstract/document/9495790/.

R. P. Reddy. (2025). "Zero Trust Architectures in Modern Enterprises: Principles, Implementation Challenges, and Best Practices,". *Int. J. Comput. Trends Technol., vol. 73, no. 6, pp. 48–57*, [Online]. Available: https://www.researchgate.net/profile/Mahammad-.

R. Zhong et al.,. (2021). "A simplified method for extracting parasitic inductances of MOSFET-based half-bridge circuit,". *IEEE Access, vol. 9, pp. 14122–14129*, [Online]. Available: https://ieeexplore.ieee.org/abstract/document/9330505/.

Ramanujam, M., Madhyastha, H. V., & R. Netravali. (2021). "Marauder: synergized caching and prefetching for low-risk mobile app acceleration,". *in Proc. 19th Annu. Int. Conf. Mobile Systems, Applications, and Services*, pp. 350–362.

Rashid, S., Bashir, F., Khanday, F. A., Beigh, M. R., & F. A. Hussin. (2021). "2-D design of double gate Schottky tunnel MOSFET for high-performance use in analog/RF applications," . *IEEE Access*, vol. 9, pp. 80158–80169. [Online]. Available: https://ieeexplore.

Rhoads, J., & A. Smith. (2024). Effectiveness of Continuous Verification and Micro-Segmentation in Enhancing Cybersecurity through Zero Trust Architecture. [Online]. Available: https://www.researchgate.net/profile/Austin-Smith-42/publication/387948985_Effec.

S. Mappouras et al.,. (2025). "A toolkit for ambulance dispatch and routing optimization using AI and GIS," in Proc. Eleventh Int. Conf. *Remote Sensing and Geoinformation of the Environment (RSCy2025),* , vol. 13816, Sep. 2025, pp. 361–367.

S. Xie et al.,. (2024). "TVDiag: A Task-oriented and View-invariant Failure Diagnosis Framework with Multimodal Data,". arXiv preprint arXiv:2407.19711, 2024. Available: https://arxiv.org/abs/2407.19711.

Sharma, P., Jindal, R., & M. D. Borah. (2022). "A Review of Blockchain-Based Applications and Challenges,". [Online]. Available: https://www.researchgate.net/publication/354853426_A_Review_of_Blockchain-Based_Applications_and_Challenges.

Song, A., Seo, E., & H. Kim. (2023). "Anomaly VAE-transformer: A deep learning approach for anomaly detection in decentralized finance,". *IEEE Access*, vol. 11, pp. 98115–98131. [Online]. Available: https://ieeexplore.ieee.org/abstract/document/10244206/.

Swain, R., Paul, A., & M. D. Behera. (2024). "Spatio-temporal fusion methods for spectral remote sensing: A comprehensive technical review and comparative analysis," . *Tropical Ecology*, vol. 65, no. 3, pp. 356–375. Available: https://link.springer.com/article.

Sytch, M., Kim, Y., & S. Page. (2022). "Supplier-selection practices for robust global supply chain networks: A simulation of the global auto industry," . *California Management Review*, vol. 64, no. 2, pp. 119–142. [Online]. Available: https://journals.sagepub.

T. Banet et al.,. (2024). "Toward improved image-based root phenotyping: handling temporal and cross-site domain shifts in crop root segmentation models,". *The Plant Phenome Journal*, vol. 7, no. 1, p. e20094. Available: https://acsess.onlinelibrary.wiley.com/.

Tabassum, M., Islam, M. I., Bristy, I. J., & M. Rokibuzzaman. (2025). "Blockchain and ERP-integrated MIS for transparent apparel & textile supply chains," . *Saudi Journal of Engineering and Technology (SJEAT)*, vol. 10, no. 9, pp. 447–456, .

Tamim, I., Saci, A., Jammal, M., & A. Shami. (2021). "Downtime-aware o-ran vnf deployment strategy for optimized self-healing in the o-cloud," . *in Proc. 2021 IEEE Global Commun. Conf. (GLOBECOM)*, pp. 1–6. [Online]. Available: https://ieeexplore.ieee.org/.

Tao, F., Akhtar, M. S., & Z. Jiayuan. (2021). "The future of artificial intelligence in cybersecurity: A comprehensive survey," . *EAI Endorsed Transactions on Creative Technologies*, vol. 8, no. 28. Available: https://pdfs.semanticscholar.org/01f0/4fd69cba1239.

U. Zurutuza. (2024). Leveraging Digital Twins and SIEM Integration for Incident Response in OT Environments. [Online]. Available: https://www.diva-portal.org/smash/record.jsf?pid=diva2:1589698.

Uriawan, W., Ramadita, R., Putra, R. D., Siregar, R. I., & R. Addiva. (2024). "Authenticate and Verification Source Files using SHA256 and HMAC Algorithms,". [Online]. Available: https://www.preprints.org/manuscript/202407.0075/download/final_file.

Valence, R., & M. F. Magada. (2025). "Supply Chain Activities and Challenges of Construction Hardware Enterprises," . *Journal of Interdisciplinary Perspectives*, vol. 3, no. 7, pp. 202–216, 2025. Available: https://www.jippublication.com/index.php/jip/article/view/4.

Y. Han et al.,. (2024). "A Novel Efficient Crash Consistency Solution Enabling Rollback Recovery for Secure NVM in Low-Power Energy Harvesting Systems,". *IEEE Trans. Dependable Secure Comput*, [Online]. Available: https://ieeexplore.ieee.org/abstract/document.

Zhu, P., Hu, J., Li, X., & Q. Zhu. (2021). "Using blockchain technology to enhance the traceability of original achievements," . *IEEE Trans. Eng. Manag., vol. 70, no. 5, pp. 1693–1707*, [Online]. Available: https://ieeexplore.ieee.org/abstract/document/9405372/.